Performance of Applied Field MPD Thruster with Various Propellants

IEPC-2019-A450

Presented at the 36th International Electric Propulsion Conference
University of Vienna • Vienna, Austria
September 15-20, 2019

Shunichiro Ide[1]
The University of Tokyo, Bunkyo-ku, Tokyo, 113-8654, Japan

Ryudo Tsukizaki[2] and Kazutaka Nishiyama[3] and Hitoshi Kuninaka[4]
ISAS / JAXA, Sagamihara, Kanagawa, 252-5210, Japan

Abstract: A quasi-steady, applied-field, rectangular magneto-plasma-dynamic thruster (AF 2D-MPD) was operated. The external magnetic field intensity is up to 400 mT and the propellant is argon and xenon. As a result, the thrust performance was improved with higher magnetic field and xenon rather than argon. In addition, a time transition of the thrust of the SF-MPD thruster with argon, xenon and hydrogen is measured using an accelerometer for confirming the quasi-steadiness of the thrust performance.

Nomenclature

J_d	=	discharge current
B_A	=	external magnetic field intensity
H	=	height of discharge chamber
F_A	=	ideal electromagnetic force
W	=	widths of discharge chamber
D	=	length of discharge chamber
I	=	impulse calibrated by impact hammer
V_d	=	discharge voltage
t_d	=	discharge time
V_c	=	charging voltage for discharge
$\dot{m}$	=	mass flow rate
F	=	measured thrust
P	=	input power
I_{sp}	=	specific impulse
η	=	thrust efficiency

I. Introduction

THE 50 kW PPE (Power and Propulsion Element) is scheduled to launch in 2022 as a first step of the Lunar Orbital Platform Gateway.[1] The input power of electric propulsion will further increase in the future. An MPD (Magneto Plasma Dynamic) thruster is suitable for inputting higher power, over 100 kW-class. Because it is lightweight and the structure is

[1] Ph.D. student, The University of Tokyo, ide@ep.isas.jaxa.jp
[2] Assistant professor, Institute of Space and Astronautical Science, ryudo@ep.isas.jaxa.jp
[3] Associate professor, Institute of Space and Astronautical Science, nishiyama@ep.isas.jaxa.jp
[4] Director General, Institute of Space and Astronautical Science, kuninaka@ep.isas.jaxa.jp

compact and simple compared with that of a hall thruster currently used mainly. However a self-induced MPD thruster (SF MPD) requires 1 MW-class power for sufficient operation: it is unrealistic in the near future. Therefore an applied-field MPD thruster (AF MPD) which operates with 10-100 kW-class power is mainly studied now as a candidate for high power electric propulsion.[2, 3] Since an AF MPD has complicated acceleration mechanism due to external magnetic field, it is essential to research on its understanding in order to optimize the performance.

The MPD thruster which has a rectangular discharge chamber (2D-MPD) has been developed in our laboratory.[4] A 2D-MPD has simpler acceleration mechanism than that of a coaxial MPD thruster, because it can apply external magnetic field in a direction directly contributing to Lorentz acceleration as shown Equation (1).

$$J_d\, B_A\, H = F_A \tag{1}$$

Therefore, a 2D-MPD is suitable for investigating the relationship between the external magnetic field and the acceleration mechanism.[5, 6] For applying stronger magnetic field with an external coil, it is easier to operating with short-time pulse than steady state operation.

In this paper, as a parametric study for understanding the acceleration mechanism of an AF-MPD thruster, we operated the applied field rectangular MPD thruster (AF 2D-MPD) applied up to 400 mT with short-time pulse. Moreover, we compared the thrust performance with argon and xenon as a typical propellant species of some electric propulsion in actual space mission for now. For confirmation of a quasi-steadiness[7] of the short-time pulse, we measured a time transition of the thrust of the SF-MPD thruster with argon, xenon and hydrogen using an accelerometer referring a few previous study.[8, 9]

II. Equipment

A. MPD Thruster

Figure 1 shows the AF 2D-MPD in this research. The discharge chamber is a rectangular solid with a height H of 8 mm, a width W of 34 mm, and a length D of 40 mm. The anodes and cathodes are made of La_2O_3-W, and three pairs of electrodes are uniformly arranged. The propellant is supplied from the rear of the discharge chamber by a fast-acting valve (FAV). The external magnetic field is generated by a Helmholtz coil using two 14-turn coils with a diameter of 80 mm on both side walls of the discharge chamber, and a uniform magnetic field of up to 400 mT is applied in the discharge chamber. An ignitor is inserted into the wall of the discharge chamber as a start of discharge. This supports electron emission by generating a spark in a booster circuit electrically independent of the thruster's electrodes.

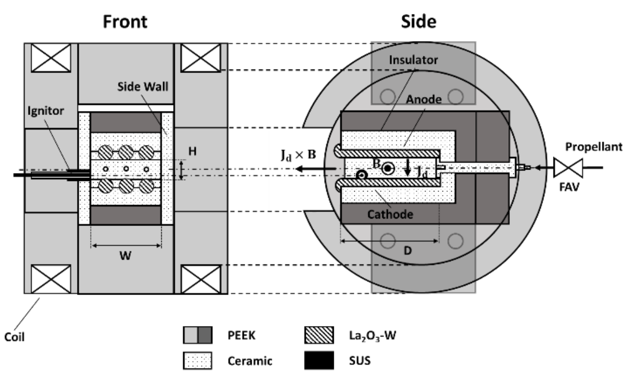

Figure 1. AF 2D-MPD thruster.

B. Power Supply

The same circuit structure is used for discharge of the thruster and operation of the coil. The circuit diagram of the power supply is shown in Fig. 2. The 12 series ultracapacitors (Maxwell BMOD0165P048C01) are used as a power source. It is switching on and off using an isolated gate bipolar transistor (IGBT) (Fuji Electric 1MBI2400VC-170E). The

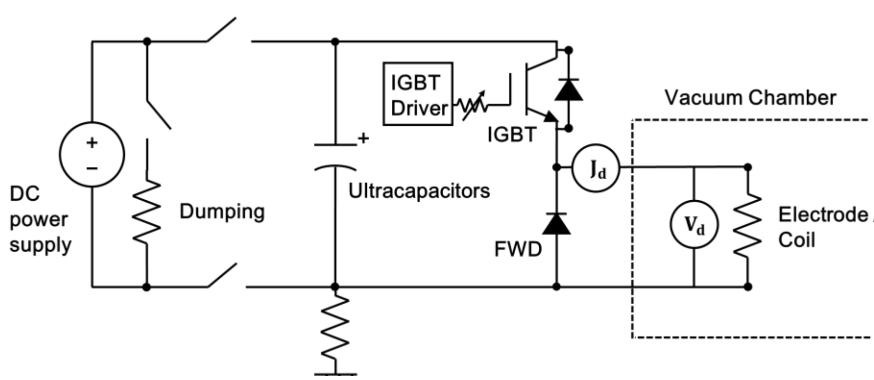

Figure 2. Circuit of power supply for thruster discharge or operating coil.

capacitors are charged up to 600 V using two DC power supply (KIKUSUI PVS 300-9) in series. In the power supply for discharge of the thruster, the discharge current J_d is measured by a non-contact sensor (LEM LF2005S) outside a vacuum chamber, and the discharge voltage V_d is measured in the vicinity of the electrodes.

C. Thrust Stand

Fig. 3 shows an outline of a gravity pendulum type thrust stand[10, 11] for measuring thrust. This research is conducted in a vacuum chamber with a length of 2.5 m and a diameter of 1.5 m in ISAS/JAXA, and the ultimate vacuum is 2×10^{-3} Pa. The thrust stand is suspended at four points with steel wire in the vacuum chamber and oscillates at about 1.5 Hz when thrust is generated. This displacement is measured by an LED sensor (Omron Z4D-F04A), and its oscillation amplitude is converted to impulse. For conversion, the calibration results previously obtained by a pseudo thrust with an impact hammer using a load cell (PCB Piezotronics 209C01) are used. The MPD thruster and the FAV are mounted on the thrust stand, and a flexible coaxial cable made by flat copper wires is connected to the electrodes and the coil from each power supply.

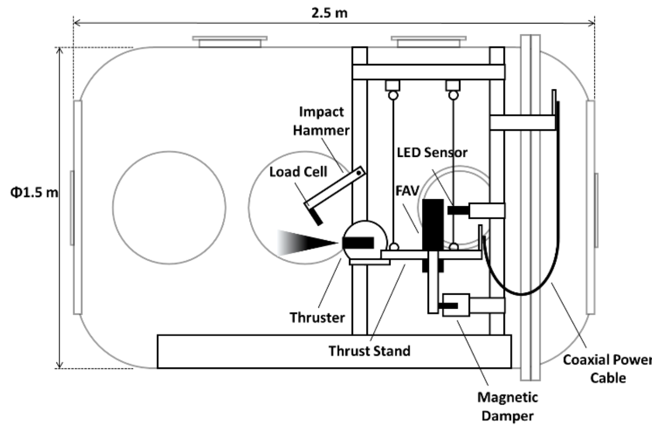

Figure 3. Thrust stand in vacuum chamber.

III. Experimental Condition

D. Operation

The operation path of the experimental devices is shown in Fig. 4. The power supplies for discharge and the coil are driven at the time determined by the pulse generator (Opt-Sciences Sapphire 9212). The propellant is once charged from the cylinder into the storage tank and supplied to the discharge chamber by the FAV driven by the FAV power supply. These devices and the ignitor are driven by triggers whose timing is determined by a delay circuit.

Fig. 5 shows the operation sequence of each experimental device. According to the gas waveform measurement in the discharge chamber using a semiconductor transducer (JTEKT PMS-5M-2 200K) the pressure of argon and hydrogen in the discharge chamber stabilizes about 5 ms after the FAV opens, 7ms in xenon. Therefore, the discharge start timing is determined considering this delay. In addition, after applying the voltage to the electrodes and the external magnetic field is sufficiently completed, the discharge is started by the igniter. Since the discharge is terminated by switching off the power supply for the electrodes, the operation time of the MPD thruster t_d can be determined by the operation time determined by the pulse generator.

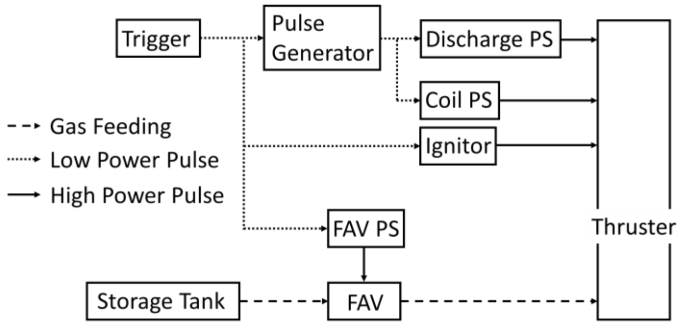

Figure 4. Operation path of experimental equipment.

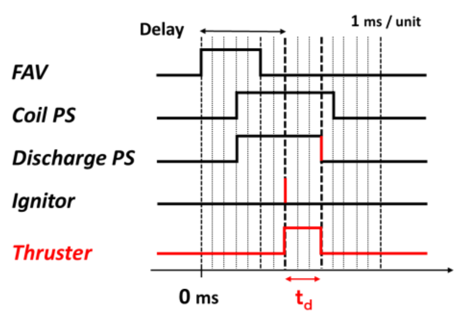

Figure 5. Operation sequence.

E. Parameters

The experimental parameters are summarized in Table 1. Since the discharge voltage and the discharge current both change when the charging voltage V_c is changed, the discharge characteristics in a wide range can be investigated. The flow rate of the propellant is uniquely determined by the pressure in the storage tank. The operation time of the thruster t_d is determined as shown Fig.5.

Table 1. Experimental condition for a) applied field effect and b) propellant species.

a)

Parameters	Values
V_c, V	100 / 120 / 150 / 180 / 200 / 230
B_A, mT	100 / 200 / 400
Propellant	Ar
$\dot{m}$, mg/s	40 / 50 / 100
t_d, ms	3.0

b)

Parameters	Values
V_c, V	200 / 230 / 250 / 270 / 300
B_A, mT	400
Propellant	Ar / Xe
$\dot{m}$, mg/s	5 / 10 / 30 / 50 / 80 / 100
t_d, ms	2.0

IV. Experimental Result

F. Characteristics of Applied Field Intensity

Fig.6 shows a) the discharge voltage V_d and b) the thrust F against the discharge current J_d of operation with argon in the condition of Table.1 a). V_d and J_d are average values during flat-top region of the discharge waveform. F is calculated by Equation (2). As B_A becomes higher, J_d decreases and V_d increases. At B_A is 400 mT, the thruster is operated with almost the same as the charging voltage V_c. The slope of the thrust F to the discharge current J_d is improved as B_A becomes stronger.

$$F = \frac{I}{t_d} \tag{2}$$

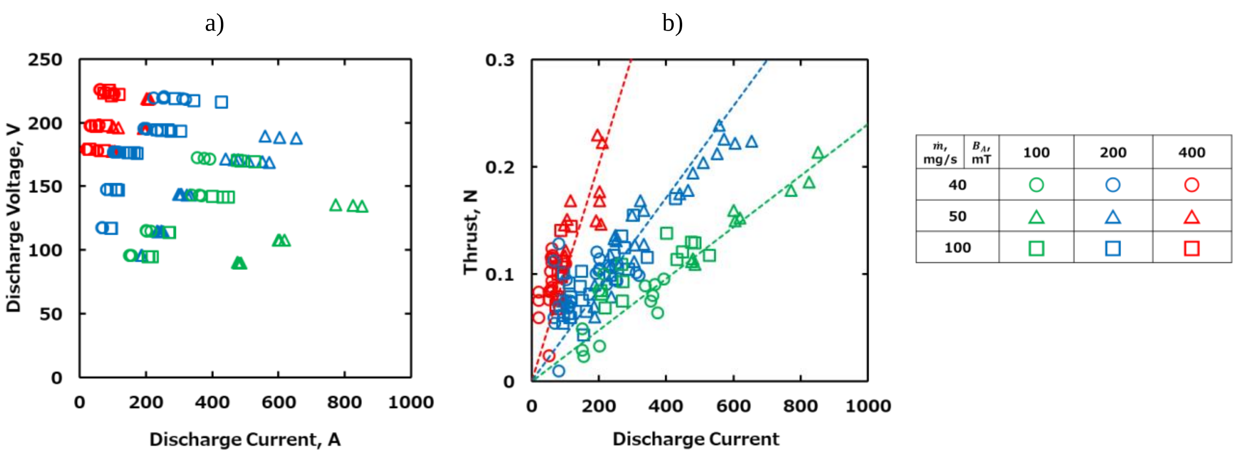

Figure 6. a) Discharge voltage and b) thrust against discharge current of operation with argon

G. Characteristics of Propellant Species

Fig.7 shows a) the discharge voltage V_d and b) the thrust F against the discharge current J_d of operation with argon and xenon in the condition of Table.1 b). The specific impulse I_{sp} and the thrust efficiency η is calculated by Equation (3)-(5).

$$P = V_d J_d \tag{3}$$

$$I_{sp} = \frac{F}{\dot{m}g} \tag{4}$$

$$\eta = \frac{F^2}{2\dot{m}P} \tag{5}$$

With xenon, the thruster is operated lower J_d and higher V_d than that with argon. About thrust performance, F is little bit higher with xenon because of higher V_d than that with argon. Decreasing the mass flow rate $\dot{m}$ to 10 mg/s, the thrust to power (F/P) is reached to 14.5 mN/kW in xenon and 9.8 mN/kW in argon.

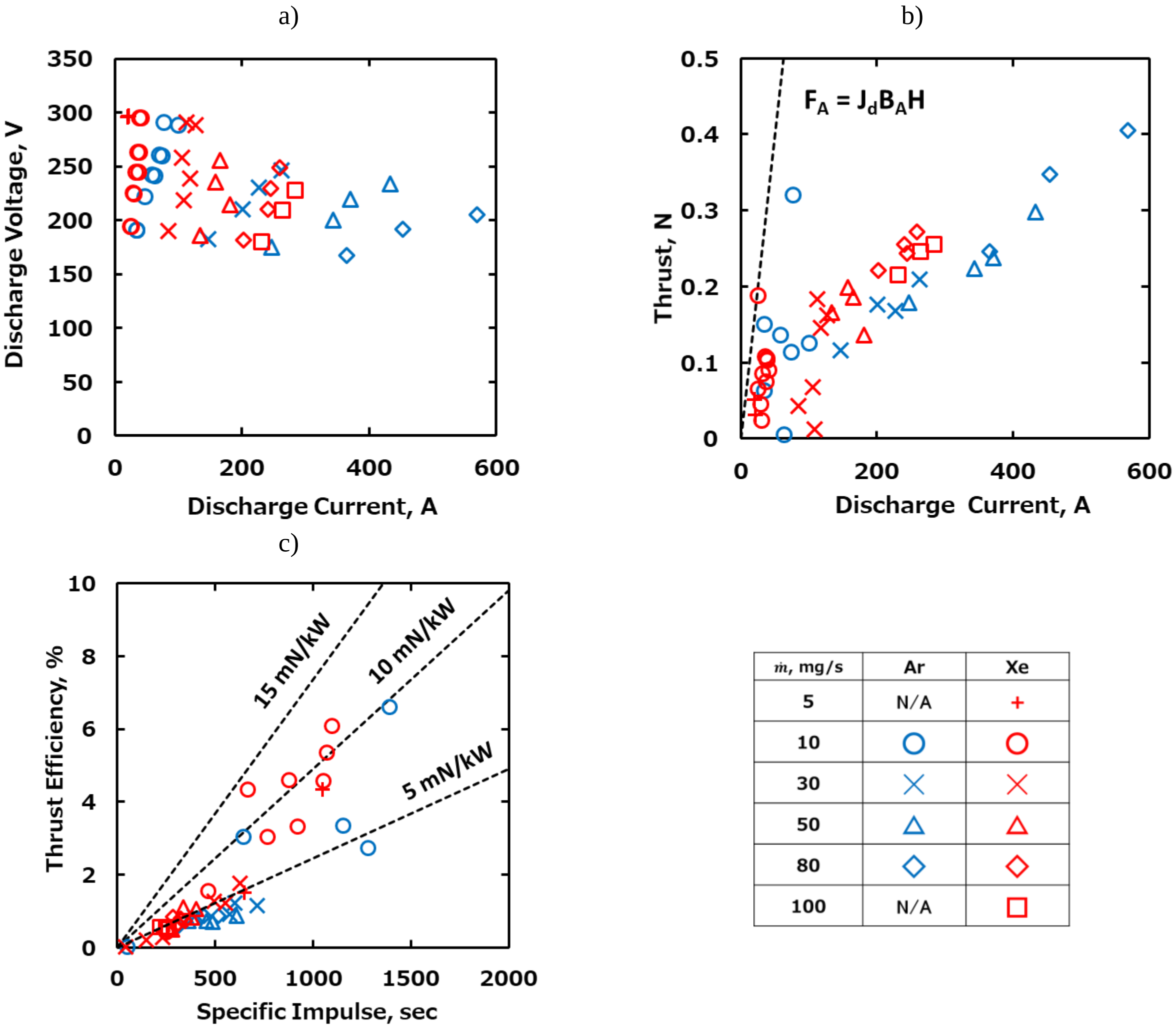

Figure 7. a) Discharge voltage and b) thrust against discharge current and c) thrust to power with argon and xenon

V. Acceleration Measurement

H. Experimental Setup

Fig.8 shows the thruster setup for measuring an acceleration of the thruster. For reducing a pulsatory motion of cables when a high current is flowing, we operate the only thruster head deployed the coils. The 2-axis accelerometer tip (Analog Devices ADXL203CE) is mounted the above of the discharge chamber. The thruster is suspended without the thrust stand as shown Fig.9. For converting the acceleration to the thrust, we calibrated by the impact hammer same as the calibration of the LED sensor in the thrust stand. The calibration result shows in Fig.10. The acceleration of X and Y axis are plotted linearly and the hammer is attacked correctly from the front of the thruster because the effect of the Y axis acceleration is negligible. We used the coefficient 1.094 of the black line, calculated X^2+Y^2, for converting the acceleration to the thrust.

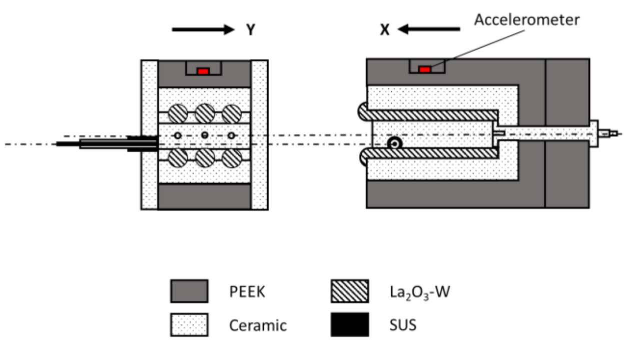

Figure 8. Thruster setup for acceleration measurement.

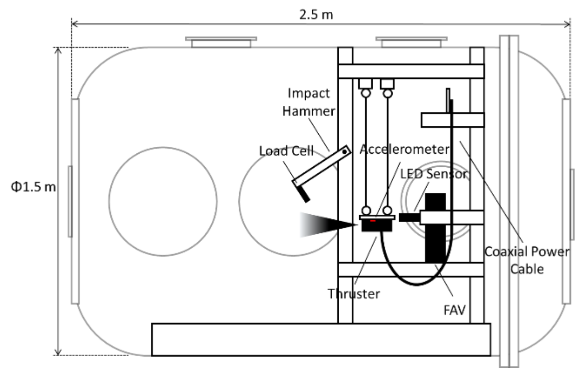

Figure 9. Suspended thruster and calibration system

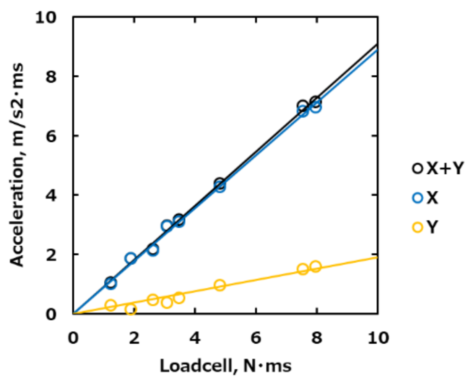

Figure 10. Calibration for Accelerometer

I. Experimental Result

The experimental condition is summarized in Table. 2. The thruster is operated without the coils and with only self-field. For emphasizing the waveform of the propellant cold-gas jet, the mass flow rate $\dot{m}$ is higher than that of the nominal operation. The result is shown in Fig.11. The blue line is the discharge current time transition, the red line is the time transition of the cold-gas jet of the propellant. The gray line is the raw data of the thrust time transition converted with Fig.10. The black line is filtered from the gray line with 1 kHz low-pass filter. From the FAV opens at 0 ms, the discharge is started by the ignitor with delaying 5 ms in argon and hydrogen or 7 ms in xenon as mentioned in chapter D. The integrated value, whose unit is Nms, of the thrust and the cold-gas jet is corresponded the impulse I measured simultaneously by the LED sensor with less than 20 % error.

The cold-gas jet is fitted with the black line and the thrust is stable with 5 and 10 ms pulse. The operation with 1 ms pulse is controversial whether it is quasi-steady state or not. Specialty, the thrust with hydrogen is 1.5-2 times in this case higher than those of argon and xenon as the same as some previous study.[12, 13] In addition, the thrust waveform with hydrogen, especially h) and i) in Fig.11, is rising with delaying about 1 ms against the discharge current waveform. It is caused that the hydrogen molecule gas is dissociated before ionization.[14, 15]

Table 2. Experimental condition for acceleration measurement.

Parameters	Values
V_c, V	230
B_A, mT	0 mT (w/o coil)
Propellant	Ar / Xe / H_2
$\dot{m}$, g/s	0.95 (Ar and Xe) / 0.3 (H_2)
t_d, ms	1.0 / 5.0 / 10.0

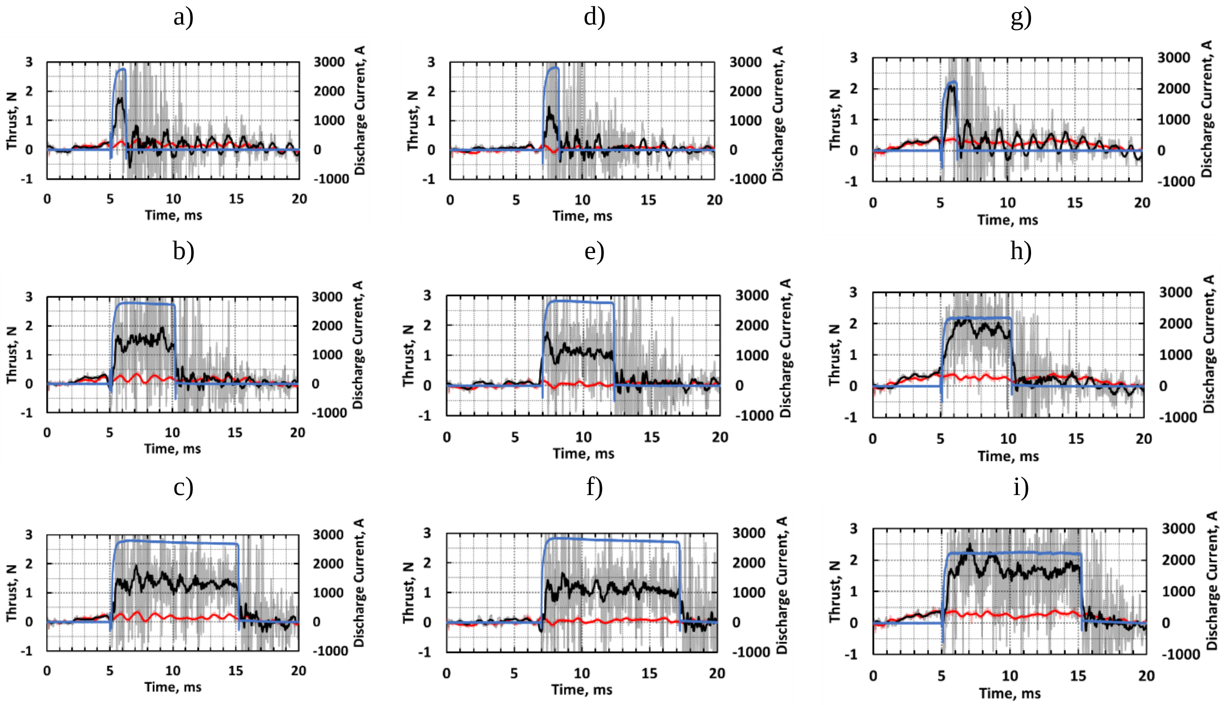

Figure 11. Thrust time transition with a)-c) argon, d)-f) xenon and g)-i) hydrogen.

VI. Conclusion

The AF 2D-MPD was operated whose the external magnetic field intensity is up to 400 mT and the propellant is argon and xenon. As a result, the thrust performance was improved with higher magnetic field and xenon rather than argon. In addition, a time transition of the thrust of the SF-MPD thruster with argon, xenon and hydrogen is measured using an accelerometer for confirming the quasi-steadiness of the thrust performance. The thrust performance was improved with higher magnetic field intensity, and xenon compared with that of argon. We confirmed the quasi-steadiness of operation with longer than 5 ms pulse and it is controversial with 1 ms pulse because of unsteady thrust time transition. With hydrogen, the delay of the thrust rising is occurred and it is speculated that a dissociation reaction of the hydrogen molecule gas is occurred before ionization.

Acknowledgments

This study was technically supported by the Advanced Machining Technology Group of the Japan Aerospace Exploration Agency.

References

[1] Herman, D., Tofil, T., Santiago, W., Kamhawi, H., Mcguire, M., Polk, J. E., Snyder, J. S., Hofer, R., Picha, F., Jackson, J., and Allen, M. : Overview of the Development and Mission Application of theAdvanced Electric Propulsion System (Aeps):Presented at the 35th International Electric Propulsion Conference,IEPC-2017-284, Atlanta, 2017.

[2] MANTENIEKS, MARISA, et al. Performance of a 100 kW class applied field MPD thruster. In: *25th Joint Propulsion Conference*. p. 2710.1989.

[3] A. Boxberger, G. Herdrich : Integral Measurements of 100 kW Class Steady State Applied-Field Magnetoplasmadynamic Thruster SX3 and Perspectives of AF-MPD Technology, Presented at the 35th International Electric Propulsion Conference

[4] Takubo, Masaya, et al. "Effect of Inter-electrode geometry on the performance of an applied-field 2D MPD thruster." 48th AIAA/ASME/SAE/ASEE Joint Propulsion Conference & Exhibit. 2012.

[5] FunakiIkko, et. al.: Electrode Configuration Effect on the Performance of a Two-Dimensional Magnetoplasmadynamic Arcjet, Journal of Propulsion and Power, Vol.14, No.6, pp. 1043-1048, 1998.

[6] Funaki, I., K. Toki, and K. Kuriki. "Electrode configuration effect on the performance of a two-dimensional magnetoplasmadynamic arcjet." Journal of Propulsion and Power 14.6 (1998): 1043-1048.

[7] Clark, K. E., & Jahn, R. G. (1970). Quasi-steady plasma acceleration. AIAA Journal, 8(2), 216-220.

[8] Kuriki, K., & Suzuki, H. (1978). Transitional behavior of MPD arcjet operation. AIAA Journal, 16(10), 1062-1067.

[9] S. Castillo and D. Tilly, "The Air Force Phillips Laboratory Multimegawatt Quasi-Steady MPD Thruster Facility", AIAA Journal 92-3158, (1992).

[10] Nicolini, D., Frigot, P., Musso, F., Cesare, S., Castorina, G., Ceruti, L., Bartola, F., Zanella, P., Ceccanti, F., Priami, L., and Paita, L., "Direct Thrust and Thrust Noise Measurements on the LISA Pathfinder Field Emission Thruster IEPC-2009-183," 31st International Electric Propulsion Conference, AIAA Paper 2009-0183, 2009.

[11] Cesare, S., Musso, F.,D'Angelo, F., Castorina, G., Bisi, M., Cordiale, P., Canuto, E., Nicolini, D., Balaguer, E., and Frigot, P.-E., "Nanobalance: The European Balance for Micro-Propulsion," 31st International Electric Propulsion Conference, AIAA Paper 2009-0182, 2009.

[12] K. Uematsu, S. Morimoto, and K. Kuriki : "MPD Thruster Performance with Various Propellants", J. Spacecraft, Vol.22, No.4, pp.412-416 (1982)

[13] J. S. Sovey and M. A. Mantenieks : "Performance and Lifetime Assessment of Magnetoplasmadynamic Arc Thruster Technology", J. Propul., Vol.7, No.1, pp.71-83 (1991)

[14] K. Mitsuo, H. Tahara, T. Kimura, Y. Kagaya, and T. Yoshikawa : "Arc Strucutre in a Coaxial Magnetoplasmadynamic Channel", 25th International Electric Propulsion Conference, IEPC-99-179, Kitakushu, Japan (1999)

[15] P. G. Mikellides : "Modeling and Analysis of a Megawatt-Class Magnetoplasmadynamic Thruster", J. Propul. Power, Vol.20, No.2, pp.204-210 (2004)